*Hum Mol Genet*. Author manuscript; available in PMC 2013 November 04.

Published in final edited form as:
*Hum Mol Genet*. 2009 November 15; 18(22): 4255–4267. doi:10.1093/hmg/ddp379.

# The interval between *Ins2* and *Ascl2* is dispensable for imprinting centre function in the murine Beckwith-Wiedemann region

**Louis Lefebvre**[1,*], **Lynn Mar**[2], **Aaron Bogutz**[1], **Rosemary Oh-McGinnis**[1], **Mohammad Mandegar**[1], **Jana Paderova**[3], **Marina Gertsenstein**[4], **Jeremy A. Squire**[3,5], and **Andras Nagy**[4]

[1]Department of Medical Genetics and Molecular Epigenetics Group, Life Sciences Institute, The University of British Columbia, Vancouver, BC, Canada V6T 1Z3

[2]Dana-Farber Cancer Institute, Boston, MA 02115

[3]Applied Molecular Oncology, Ontario Cancer Institute, Princess Margaret Hospital, and Department of Medical Biophysics, University of Toronto, Ontario M5G 2M9

[4]Samuel Lunenfeld Research Institute, Mount Sinai Hospital and Department of Medical Genetics, University of Toronto, Toronto, Ontario M5G 1X5

## Abstract

Imprinted genes are commonly clustered in domains across the mammalian genome, suggesting a degree of coregulation via long-range coordination of their monoallelic transcription. The distal end of mouse chromosome 7 contains two clusters of imprinted genes within a ~1 Mb domain. This region is conserved on human 11q15.5 where it is implicated in the Beckwith-Wiedemann syndrome. In both species, imprinted regulation requires two critical *cis*-acting imprinting centres, carrying different germline epigenetic marks and mediating imprinted expression in the proximal and distal sub-domains. The clusters are separated by a region containing the gene for tyrosine hydroxylase (*Th*) as well as a high density of short repeats and retrotransposons in the mouse. We have used the Cre-*lox*P recombination system *in vivo* to engineer an interstitial deletion of this ~280-kb intervening region previously proposed to participate in the imprinting mechanism or to act as a boundary between the two sub-domains. The deletion allele, $Del^{7AI}$, is silent with respect to epigenetic marking at the two flanking imprinting centres. Reciprocal inheritance of $Del^{7AI}$ demonstrates that the deleted region, which represents more than a quarter of the previously defined imprinted domain, is associated with intrauterine growth restriction in maternal heterozygotes. In homozygotes, the deficiency behaves as a *Th* null allele and can be rescued pharmacologically by bypassing the metabolic requirement for TH *in utero*. Our results show that the deleted interval is not required for normal imprinting on distal Chr 7 and uncover a new imprinted growth phenotype.

[*]Correspondence to Louis Lefebvre, louis.lefebvre@ubc.ca, tel: 604-822-5310, fax: 604-822-5348.
[5]Present address: Department of Pathology and Molecular Medicine, Queen's University, Kingston, Ontario K7L 3N6

## Introduction

The distal end of mouse chromosome 7 (Chr 7) contains a large cluster of imprinted genes, located in cytogenetic band 7F5. This domain defines a ~1Mb region rich in imprinted transcripts (1). The region shares syntenic homology with human 11p15, where abnormal regulation of imprinting is associated with the Beckwith-Wiedemann syndrome (BWS, OMIM 130650), a congenital overgrowth syndrome (2, 3). Comparative analyses between mouse and human suggest a high degree of conservation, not only of the genomic organization and sequences of the orthologous regions, but also of the imprinted expression of several key genes within these clusters (4–6). Genetic studies on distal Chr 7 have therefore provided important models for BWS, while contributing to our knowledge of the general mechanism and function of imprinting in mammals.

Our current understanding of the regulation of imprinting on distal Chr 7 suggests that two imprinting centers (ICs) are responsible for the reciprocal imprinting of two sub-domains within this cluster. In the proximal sub-domain, a CpG-rich sequence located ~2 kb upstream of the *H19* gene acquires a DNA methylation imprint in sperm but not in eggs (7–9). This sequence termed *H19* DMR or IC1 acts as an imprinting centre (10) and regulates monoallelic expression of nearby genes via two different mechanisms. DNA methylation of the paternal IC1 leads to silencing of *H19* in *cis* as well as paternal allele-specific expression of at least two protein-coding genes, *Igf2* and *Ins2*, via a CTCF-dependent insulator or boundary element acting exclusively on the umethylated maternal allele (11–14).

The telomeric (distal) sub-domain is also marked by a differentially methylated CpG-rich region, but here the germline imprint is exclusively inherited from the oocyte. Located within intron 10 of *Kcnq1*, this sequence termed *KvDMR1* or IC2 acts as a promoter for the large non-coding RNA *Kcnq1ot1* (15, 16). Expression of *Kcnq1ot1* exclusively from the paternal homolog has been linked to the silencing of several protein-coding genes in *cis*, such as *Cdkn1c, Phlda2,* and *Ascl2* (15–17). These genes are consequently imprinted and expressed preferentially from the maternal homolog. Imprinted monoallelic expression in this distal sub-domain is therefore thought to be under the regulation of *Kcnq1ot1* transcription and/or the transcript.

Whereas several studies have focused on the function of IC1 and IC2, their independent imprinting at ectopic genomic locations, and the transcripts they each regulate, very little is known about possible interactions between the two imprinted sub-domains in the context of distal Chr7 (10, 17–19). The linkage between these two imprinting centres is conserved in eutherians and provides a model to study long-range interactions between centres as well as to address the possible presence of boundaries or insulators defining the range of action of each centre. In the mouse, the interval between *Ins2* (20), located at the distal end of the known IC1-regulated domain, and *Ascl2*, the most proximal transcript known to be regulated by IC2 (17, 21), represents close to a third of the entire distal 7 domain. This region contains a single known protein-coding gene, *Th*, which codes for tyrosine hydroxylase, the rate-limiting enzyme in the synthesis of catecholamines.

We have used an *in vivo* Cre-*lox*P approach to engineer a ~280-kb deletion of the IC1-IC2 intervening region. Proximal and distal breakpoints of this deletion were defined by targeted *lox*P site insertions next to the *Ins2* and *Ascl2* loci. From Cre-mediated trans-allelic recombination in spermatocytes we recovered the reciprocal deletion ($Del^{7AI}$) and duplication ($Dp^{7AI}$) alleles. We show here that the initiation and maintenance of epigenetic marking at IC1 and IC2 by DNA methylation are not affected by this deletion. Both maternal and paternal deletion heterozygotes are viable but maternal heterozygotes exhibit an intrauterine growth retardation phenotype. We also report the post-implantation lethality of $Del^{7AI}/Del^{7AI}$ homozygotes and the developmental rescue of this phenotype by provision of exogenous L-DOPA *in utero* during gestation. These results provide genetic evidence for the absence of new developmentally required genes in this large region of Chr 7 and suggest that deletion homozygotes phenocopy a *Th* deficiency with respect to developmental survival.

## Results

### Unique features of the *Ins2-Ascl2* interval

The paternally expressed imprinted genes *Igf2* and *Ins2* belong to an ancient chromosomal paralogy group linking genes for insulin-related proteins (IGF) to members of the aromatic amino acid hydroxylase family (AAAH) in vertebrates (22). This group extends to the genes for the *achaete-scute* family of transcription factors (ASCL) in several vertebrate genomes. In the mouse genome, *Igf2-Ins2-Th-Ascl2* maps to the distal end of Chr 7, whereas the paralogs *Igf1-Pah-Ascl1* are present on Chr 10. Members of the first group are regulated by genomic imprinting, but this is not the case for the paralogs on Chr 10. The same regions are present on human chromosomes 11 and 12 respectively (23). Although both *IGF2* and *INS* are imprinted in human (24–26), there is still no definitive evidence for the imprinting of *TH* or *ASCL2,* which are both maternally expressed in the mouse placenta (21, 27).

We have defined two intervening regions or gaps in these paralogy regions, gap 1 (IGF-AAAH) and gap 2 (AAAH-ASCL) and analyzed their structure and sequence composition in seven vertebrate genomes (Fig. S1A of Supplementary Material). Our analysis shows that the greatest variation in gap sizes is observed in gap 1 of the mouse *Igf2-Ins2* to *Th* region (Fig. S1B). Most of this size increment is attributable to a significant increase in the content of repetitive elements, notably LINEs and LTR elements (Fig. S1C). Compared to the gap 1 of the IGF1-PAH paralogy region, there is also more variation in the GC content of the IGF2-INS-TH region between non-imprinting (chicken, zebrafish) and imprinting mammalian species (mouse, human, dog, cow) (Fig. S1C). Other unique features of the mouse *Igf2-Ins2-Th-Ascl2* region which have been previously described include the presence of a large block of tandem repeats of a 30-bp sequence (28), as well as the identification by circular chromosome conformation capture of five sequences in gap 1 physically interacting with the unmethylated maternal IC1 (asterisks in Fig. 1A) (29). To address the function of these features in the regulation of imprinting on distal Chr 7, we have engineered a deletion of the *Ins2* to *Ascl2* interval.

### New deletion and duplication alleles on distal Chr 7

We have used the Cre-*lox*P site-specific recombination system to introduce a chromosomal deletion removing the entire region located in between the sub-domains regulated by the imprinting centres IC1 and IC2. The deleted interval of ~280-kb is flanked by the *Ascl2* and *Ins2* loci, respectively (Fig. 1A). For this purpose we designed bipartite *PGK-neo*-pA cassettes in which *lox*P sites flank only the *PGK* promoter or only the *neo*-pA element, and generated targeting vectors carrying these complementary selectable markers (30). Gene targeting in R1 ES cells (31) was used to introduce *lox*P-carrying insertional mutations at the *Ascl2* and *Ins2* loci (Fig. 1B–1C). The proximal breakpoint is defined by a *lox*P site inserted 2.56 kb telomeric of *Ins2* (*Ins2*$^{tm1Nagy}$ allele, referred to below as the *I2* allele; Fig. 1B). We previously described the construction and targeting of this allele at the *Ins2* locus (30). For the distal breakpoint of the deletion we targeted a *lox*P site 4.34 kb centromeric to *Ascl2* (*Ascl2*$^{tm2Nagy}$ allele, referred to below as the *M2* allele; Fig. 1C). The conditionality of the *neo* cassette was demonstrated by transient expression of Cre recombinase in these cell lines and the characterization of G418-sensitive *Ascl2*$^{+/M2loxP}$ cell line variants (*Ascl2*$^{tm2.1Nagy}$ allele) with a simple *PGK*-*lox*P insertion (Fig. 1C). We generated chimeras with ES cell clones carrying the individual *M2* and *I2* insertion alleles and obtained germline transmission for both of these alleles. In each case, the heterozygous and homozygous mice are viable and fertile, with no obvious phenotype, suggesting that the *M2* and *I2* alleles constitute phenotypically silent insertions.

The availability of *Ascl2*$^{M2/M2}$ and *Ins2*$^{I2/I2}$ homozygous mouse lines offered the possibility of generating the desired deletion *in vivo*, using a Cre *trans*-recombination in spermatocytes. This strategy, referred to as TAMERE (TArgeted MEiotic REcombination), was used previously to generate reciprocal deletion and duplication alleles within the *Hoxd* locus (32, 33). It is based on the use of the *Sycp1*-Cre transgenic mouse line expressing the Cre recombinase in primary spermatocytes, driven by the promoter for the synaptonemal complexe protein 1 gene, *Sycp1* (34, 35). First, we generated *Ascl2*$^{M2/+}$ *Sycp1*-Cre double transgenic males by crossing *Ascl2*$^{M2/M2}$ females with males hemizygous for the *Sycp1*-Cre transgene. As previously reported (35), we observed ubiquitous somatic excision of the *M2* allele to form *M2loxP* in some of the progeny (1 in 11 males analyzed, Fig. S2A, Supplementary Material). To confirm that the double transgenic males selected for the next cross carry a functionally active Cre transgene, we only bred the *Sycp1*-Cre positive males showing no sign of somatic excision of the *M2* allele.

Second, we crossed *Ins2*$^{I2/I2}$ homozygous females to one of the *Ascl2*$^{M2/+}$ *Sycp1*-Cre double transgenic male. For this cross, we observed Cre-mediated conversion of *M2* to *M2loxP* in 10/11 progeny heterozygous for the *lox*P site insertion at *Ascl2*, confirming efficient germline activity of the Cre transgene in this particular male (Fig. S2B, Supplementary Material). Three of these mice were confirmed triple transgenic males with the *Ascl2*$^{+/M2loxP}$ *Ins2*$^{I2/+}$ *Sycp1*-Cre genotype. In these males, the *lox*P site are therefore present in a *trans* configuration, one on each parental Chr 7 homolog.

In the final crosses, wild-type outbred females were mated with males trans-heterozygous for the *lox*P site insertions and carrying the *Sycp1*-Cre transgene (Fig. 2A). Recombination between these non-allelic *lox*P sites, located ~280 kb apart, is expected to generate two

reciprocal recombination products: a deletion (*Del*$^{7AI}$) and a duplication (*Dp*$^{7AI}$) of the intervening sequences (Fig. 2B). From these crosses, viable mice heterozygous for the deletion or duplication alleles were recovered at weaning, as initially confirmed by allele-specific PCR assays (Fig. 2C). In total, we analyzed six litters from two transgenic males. From a total of 84 progeny genotyped at weaning, we obtained 13 +/*Del*$^{7AI}$ and 16 +/*Dp*$^{7AI}$ paternal heterozygous pups (Supplementary Table S1, cross 1).

The structure of the *Dp*$^{7AI}$ duplication allele was confirmed by Southern blot analysis of genomic DNA samples isolated from heterozygous progeny and wild-type litter mates. In all heterozygous +/*Dp*$^{7AI}$ samples analyzed, *Ascl2* and *Ins2* genomic probes internal to the *lox*P-flanked region hybridized to a novel, common, mutant restriction fragment (Supplementary Fig. S3A and B). This is consistent with the repetition of *Ascl2* 3′-flanking sequences next to the *Ins2 lox*P site. We also amplified and sequenced this newly formed junction between the 5′ end of *Ins2* and the 3′ end of *Ascl2*. The DNA sequence obtained confirmed the presence of a single junctional *lox*P site, flanked by the expected linker sequences from the targeting vectors and the genomic sequences of the appropriate arms of homology (Supplementary Fig. S3C).

All the +/*Dp*$^{7AI}$ mice obtained from TAMERE are phenotypically indistinguishable from their wild-type litter mates and the same is true upon maternal and paternal transmission of the allele from +/*Dp*$^{7AI}$ mice (L.L., unpublished data). The duplication allele has not been characterized further for the present study.

## The *Del*$^{7AI}$ allele brings the *Ascl2* and *Ins2* loci in close proximity

We analyzed the structure of the *Del*$^{7AI}$ deletion allele by Southern blot analysis, using genomic probes from the *Ascl2* and *Ins2* loci, flanking and external to the deletion breakpoints. All the restriction enzyme digests tested present a new fragment, unique to the *Del*$^{7AI}$ allele and shared by the two probes (Fig. 3A). Further molecular evidence for the deletion of Chr 7 sequences was provided by confirming the hemizygosity of a polymorphic marker internal to the deleted region in +/*Del*$^{7AI}$ heterozygous embryos at E13.5 (Supplementary Fig. S4). Some of these E13.5 embryos were also used to culture primary embryonic fibroblasts, which were grown in absence or presence of G418. All the G418-resistant fibroblast cultures were from +/*Del*$^{7AI}$ embryos, demonstrating that a functional PGK-*loxP-neo*-pA marker had been re-formed at the recombination junction (Supplementary Fig. S5). These fibroblasts also provided a source of metaphase spreads for DNA-FISH experiments using as probes genomic PAC clones from regions proximal (*H19*), internal (*Th*) or distal (*Phlda2*) to the deletion (see Fig. 1A for probe positions). Whereas the internal *Th* probe gave a signal on both Chr 7 homologs in wild-type cells (Fig. 3B, right panel), only one of the two *H19*-positive Chr 7 homologs also gave a signal for the internal *Th* probe in *Del*$^{7AI}$ heterozygous cells (Fig. 3B, left panel). The integrity of the Chr 7 region telomeric to the *Ascl2 lox*P site in the *Del*$^{7AI}$ allele was also confirmed with the distal *Phlda2* probe. Here again, the flanking probe gave a signal on both Chr 7 homologs, only one of which also carries the *Th* locus, identifying it as the wild-type Chr 7 (Fig. 3B, middle panel). Together our results confirm the structure of the deletion allele which brings *Ins2* and *Ascl2* in close proximity.

## Growth retardation in maternal *Del*$^{7AI}$ heterozygotes

Although the heterozygous mutant progeny obtained by TAMERE from triple-transgenic males were viable and fertile, the inherited deletion allele was generated *de novo* in primary spermatocytes and did not go through reprogramming in the male germline. Therefore, we first assessed the phenotype associated with the deletion *Del*$^{7AI}$ through reciprocal crosses between wild-type mice and the +/*Del*$^{7AI}$ progeny obtained by TAMERE. The distal Chr 7 imprinted domain contains several developmentally important genes, including *Igf2* (36, 37), *Cdkn1c* (38–40), *Phlda2* (41), and *Ascl2* (21, 42). Consequently, disruption of epigenetics regulation at IC1 and/or IC2 is expected to yield distinct and characteristic embryonic or early postnatal phenotypes. Paternal +/*Del*$^{7AI}$ and maternal *Del*$^{7AI}$/+ heterozygotes were recovered at the expected frequency at weaning from the carrier parents (Supplementary Table S1, crosses 2 and 3). No abnormalities or growth differences were observed in the paternal heterozygotes (Fig. 4A and B), but maternal transmission of the deletion allele caused intrauterine growth restriction in mutant progeny, which were almost 20% smaller than their wild-type littermate at birth on average (Fig. 4A). This growth difference is maintained to weaning, with no sign of catch up by the mutants (Fig. 4C). Both *Del*$^{7AI}$/+ and +/*Del*$^{7AI}$ heterozygotes grow to become mature and fertile adults.

We then assessed the compatibility of the deletion allele with erasure and re-establishment of parental imprints by taking the mutation thought the opposite germline. This was achieved by crossing paternal heterozygous +/*Del*$^{7AI}$ females or maternal heterozygous *Del*$^{7AI}$/+ males with wild-type mice. Here again, deletion heterozygotes were recovered at the expected Mendelian ratio with no progeny loss in utero (Supplementary Table S1, crosses 4 and 5).

## Normal imprinting at IC1 and IC2 in deletion heterozygotes

Our breeding data suggested that the deletion of the large region flanked by the IC1- and IC2-regulated imprinted sub-domains is silent with regard to epigenetic regulation on distal Chr 7. To assess the effect of *Del*$^{7AI}$ on the imprinting at IC1 and IC2 we looked at imprinted expression of the non-coding RNAs and DNA methylation marks at each imprinting centers in wild-type and reciprocal heterozygous *Del*$^{7AI}$ embryos (Figures 5 and 6). For allele-specific studies, we crossed *Del*$^{7AI}$ heterozygotes with mice from a congenic mouse line, derived in our laboratory, and carrying the *M. m. castaneus* variant (denoted C) of distal Chr 7 in the 129S1 background. From these crosses, we obtained reciprocal wild-type (C/+ and +/C) and *Del*$^{7AI}$ heterozygous (C/Δ and Δ/C) embryos with expressed polymorphisms at *H19* and *Kcnq1ot1*. The allele-specific RT-PCR analyzes confirmed exclusive maternal expression of *H19* (Fig. 5B) and paternal expression of *Kcnq1ot1* (Fig. 6B). Partial DNA methylation at the imprinting centres was first demonstrated by Southern blot analysis of embryonic genomic DNA (Fig. 5C and 6C) and the parent-of-origin imprints at IC1 and IC2 were confirmed in reciprocal *Del*$^{7AI}$ heterozygotes by bisulfite conversion and sequencing, using SNPs between *castaneus* and *domesticus* variants to assign parental origin of each sequenced strand (Fig. 5D and 6D). Our results therefore show that both paternal and maternal primary epigenotypes are unperturbed by the deletion allele and that the deleted region is dispensable for imprinting at IC1 and IC2.

### TH deficiency phenotype in *Del$^{7AI}$* homozygotes

In order to assess the phenotypic consequence of homozygous loss of the deleted region, we performed intercrosses between *Del$^{7AI}$* heterozygotes. Live *Del$^{7AI}$*/*Del$^{7AI}$* pups were not recovered from such crosses, suggesting an embryonic lethality phenotype (Fig. 7A). Analysis of litters at E10.5 and E14.5 showed that the homozygous mutant embryos are viable at those stages, although abnormalities suggestive of cardiovascular defects were often observed in older embryos (Fig. 7B). These observations, together with the late developmental or perinatal lethality, were reminiscent of the phenotype described by several groups for the *Th*-null embryos (43, 44). This developmental requirement for tyrosine hydroxylase can be shunted pharmacologically by administration of L-DOPA, the product of the reaction, in the diet of the mother during gestation. This phenotypic rescue was attempted for the *Del$^{7AI}$* allele by repeating heterozygous crosses and adding L-DOPA to the drinking water of the pregnant females throughout gestation. Using this protocol, we were able to recover viable *Del$^{7AI}$*/*Del$^{7AI}$* pups (Fig. 7A and C). These TH-deficient mice are indistinguishable from heterozygous and wild-type litter mates at birth, but failed to thrive postnatally and died before weaning (Fig. 7D). The phenotypic characteristics and metabolic rescue of the homozygous *Del$^{7AI}$*/ *Del$^{7AI}$* mutants generated here suggest that this large deletion is a phenocopy of a *Th* null allele with regard to the developmental phenotype and that the deleted region is thus devoid of additional genes, other than *Th*, required for normal development.

Recent results suggested that *Th* is imprinted in the developing placenta, and preferentially expressed from the maternal allele (27). This observation raises the possibility that the imprinted growth retardation phenotype noted only in *Del$^{7AI}$*/+ maternal heterozygotes is caused by loss of TH function during development. We directly tested this hypothesis by asking whether L-DOPA provision to pregnant *Del$^{7AI}$* heterozygous females is able to rescue to growth defects of their mutant progeny. Our results showed that L-DOPA was not able to rescue the IUGR phenotype since *Del$^{7AI}$*/+ progeny are indistinguishable from those obtained from non-treated females at birth (Fig. 4A) and up to weaning (Fig. 4D). Our results suggest that loss of imprinted *Th* is not responsible for IUGR. Further studies will address the roles of IC2-regulated genes in this novel imprinted phenotype.

## Discussion

Several studies have provided annotation and comparative sequence analysis data for the distal Chr 7 imprinted region. Motivated by the importance of the region in BWS and as a model for imprinted gene regulation in mammals, these have addressed the conservation of transcripts and intergenic sequences between mouse, human, chicken, zebrafish, and marsupials (5, 6, 23, 45–47). Other analyses have focused on the evolution of specific gene families in the region, notably the insulin-like coding genes and the aromatic amino acid hydroxylase families (22). In the context of our study, two different aspects of this work are of particular relevance: (*i*) the function of the IC1-IC2 intervening region and (*ii*) the evolution of imprinting at IC1 and IC2.

We present here the generation and description of the largest interstitial deletion within the mouse ortholog of the Beckwith-Wiedemann syndrome (BWS) region. Deletion of the gap

1-*Th*-gap 2 intervening region in the *Igf2-Ins2-Th-Ascl2* paralogy region is silent for primary germline imprinting at the flanking imprinting centres IC1 and IC2. We show that $Del^{7AI}$ is associated with an imprinted intrauterine growth retardation phenotype and that homozygous mutants fail to develop to term. Furthermore, we show that this lethality but not not growth defects can be pharmacologically rescued by bypassing the developmental requirement for the deleted *Th* gene. Our work has important implications for the regulation and role of imprinting on distal Chr 7.

We have uncovered an imprinted intrauterine growth retardation (IUGR) phenotype observed only in maternal heterozygotes. Since a key regulator of embryonic growth, *Igf2,* is expressed from the paternal chromosome, it is unlikely that the maternal $Del^{7AI}$ allele exerts its effect via *Igf2*. Trans effects have been previously described in specific allele combinations at the *Ins2* locus (48), but because of functional redundancy with *Ins1*, *Ins2*-deficient mice have no reported abnormal phenotype (49, 50). Another possibility was that $Del^{7AI}$/+ embryos are growth retarded due to absence of the maternal *Th* allele. The genomic organization of human *TH* relative to the IC1 and IC2 sub-domains is conserved in humans, although it is located closer to the insulin locus *INS* due to deletion-insertion rearrangements. In human, mutations in the *TH* gene have been identified in patients with recessive juvenile distonia, a parkinsonian-like condition referred to as Segawa syndrome (OMIM 605407) (51). The genetic evidence therefore suggests that the *Th/TH* locus is not regulated by genomic imprinting, despite its genomic location. However, recent evidence suggests that *Th* is preferentially expressed from the maternal allele in the mouse placenta (27). However our inability to rescue the IUGR phenotype by provision of L-DOPA during development and the results of previous studies on *Th*-deficient mice which have not reported any abnormalities in the heterozygotes (27, 43, 44) all argue against a role for loss of imprinted *Th* in this phenotype.

Finally, another possibility for the phenotype of $Del^{7AI}$/+ embryos could be the partial disruption of expression of any one of the maternally-expressed genes of the IC2 sub-domain. Those which have been implicated in the regulation of embryonic growth and placental function include *Ascl2* (42), *Cdkn1c* (52), and *Phlda2* (41). Of these, downregulation of *Ascl2* or upregulation of *Cdkn1c* could be expected to lead to the observed IUGR phenotype, for instance via the deletion of specific enhancer or silencer elements regulating these genes. A similar although perhaps less pronounced growth deficiency was previously described in mice expressing IC2-regulated genes biallelically following deletion of the paternal *Kcnq1ot1* promoter (17).

Most known genes in the region, including *Ascl2*, *Th*, *Ins2*, *Igf2*, and *H19,* are all transcribed from the (−) strand of the mouse genome sequence. Other than the *Th* mRNA, few transcripts originating from either strand have also been described or annotated in the *Ascl2-Ins2* interval. The current mouse build (Ensembl release 54) annotates a transcript from the (+) strand (cDNA clone AK139090), located 40 kb proximal of *Th* (gene EG624121). This predicted transcript is made of 68% sequences from repetitive elements, LINE 1 and LTR elements, and codes for a predicted protein of unknown function and without homology to known proteins. The developmental rescue of $Del^{7AI}$ homozygotes by

L-DOPA confirms that the product of this gene does not perform an essential developmental function.

Analysis of the *Del*$^{7AI}$ allele narrows down the candidate region of cis-acting elements that are required for the imprinting of IC2 itself. This sequence is methylated during oogenesis but is unmethylated in the male gamete. These differential gametic epigenotypes are thought to be directly responsible for the imprinted, paternal-allele specific transcription of the *Kcnq1ot1* ncRNA, and indirectly required for the monoallelic paternal silencing of all protein-coding genes in the region. With this current model, two critical events remain to be explained namely the mechanisms for the oocyte-specific acquisition of a DNA methylation imprint at IC2, and the establishment of a silent chromatin domain from the unmethylated paternal IC2 in *cis*. Two previous studies have tested the ability of large transgenic constructs from the IC2 domain to recapitulate the imprinted regulation seen at the endogenous locus. In the first study, a 260-kb BAC transgene containing the *Cdkn1c* gene and the 3′ end of the *Kcnq1* gene, extending to IC2, failed to exhibit allele-specific imprinted expression of *Cdkn1c* (53). In the second study, a 800-kb YAC covering the entire IC2 domain with its centromeric end overlapping with roughly half of our *Del*$^{7AI}$ deletion, showed faithful imprinting of *Phlda2*, *Slc22a18, Kcnq1* and *Cdkn1c*, but failed to exhibit allele-specific imprinted expression of *Tssc4* and *Ascl2* (19). IC2 function itself was not perturbed in our study of *Del*$^{7AI}$. However, together with the results of these transgenic studies, our results raise the possibility that additional control elements, perhaps towards the telomeric end of the IC1-IC2 interval, may be critical to maintain imprinting of at least a few of the IC2-regulated genes, a possibility which will require future investigation.

## Materials and Methods

### Complementary recyclable *PGK-neo*-pA cassettes

Two complementary *PGK-neo*-pA cassette were used to insert *lox*P sites defining the breakpoint of the deletion on Chr 7, while providing a positive, dominant selection for a Cre-mediated recombination between these sites. The construction of these two partially recyclable cassettes, *lox*P-*PGK*-*lox*P-*neo*-pA and *PGK*-*lox*P-*neo*-pA-*lox*P has been described previously (30).

### Targeting vectors, alleles and Southern blot analyses

The targeting vector to generate the *I2* allele (pI2TV) as well as the description of G418$^{r}$ R1 ES cell lines carrying the *I2* allele (*Ins2*$^{I2}$, or *Ins2*$^{tm1Nagy}$) and the G418$^{s}$ *I2loxP* variants obtained by transient Cre production (*Ins2*$^{I2loxP}$, or *Ins2*$^{tm1.1Nagy}$) have been described previously (30). To construct the targeting vector for the *Ascl2*$^{M2}$ allele, a 4.1-kb *Eco*RV-*Eco*RI fragment of *Ascl2/Mash2* 3′ flanking sequences was subcloned from the 129/Sv genomic clone 19ER1 (42), into pBluescript II KS+ cut with *Eco*RV and *Eco*RI. The first *Nco*I site 3′ of exon 3 of *Ascl2* was destroyed by partial digestion and blunt ended with T4 DNA polymerase. In pM2TV, the *PGK*-*lox*P-*neo*-pA-*lox*P cassette was inserted as a blunt *Eco*RI-*Hind*III fragment into the blunted 3′ *Nco*I site, located 4.3 kb downstream of the end of exon 3 of *Ascl2*, such that both genes were in the same transcriptional orientation. In this vector, the *Eco*RI site 5′ of the *PGK* promoter is regenerated at the junction with the 3.06-

kb 5′ arm of homology from *Ascl2* genomic sequences. In the *M2loxP* allele obtained by transient Cre expression in $Ascl2^{+/M2}$ cells, the *neo*-pA of *M2* is excised, leaving behind a *PGK-lox*P insertion. Positive targeted *M2* clones and excised *M2loxP* clones were screened by Southern blotting of *Eco*RI-digested ES cell genomic DNA and hybridization with flanking and internal probes (Fig. 1B, probe A1: 1.4-kb *Eco*RI-*Xho*I fragment; probe A2: 1.05-kb *Nco*I-*Eco*RI fragment, the 3′ arm of the *M2* targeting vector pM2TV). Excision of *M2* to *M2loxP in vivo* in *Sycp1*-Cre transgenic males was monitored by *Kpn*I digestion of genomic DNA samples and hybridization with probe A3 (0.6-kb *Kpn*I-*Nco*I fragment). *Kpn*I sites flank the *M2* insertion site and yield bands of 0.9, 1.4, and 2.5-kb for the wild-type *Ascl2* locus, the *M2loxP* and the *M2* alleles, respectively.

For the analysis of progeny from heterozygous crosses (Fig. 7C), genomic DNA was digested with *Eco*RV and the Southern blot membrane was hybridized with the 1.6-kb *Eco*RV-*Hind*III fragment from the 3′ flanking region of *Ascl2*. Hybridizing bands are 5.2 kb for the wild-type allele and 9.7 kb for $Del^{7AI}$.

## ES cell culture and electroporation

The mouse embryonic stem cell line R1 (31) was maintained, expanded and electroporated as described (54). For selection the ES medium was supplemented with G418 (Sigma G9516) at 150 μg/ml. The *PGK-neo*-pA cassettes were first tested by electroporation of R1 cells with 20 μg of p*PGK-lox*P-neo-pA-*lox*P and p*lox*P-*PGK-lox*P-*neo*-pA, digested with *Eco*RI, followed by G418 selection. For the two rounds of targeting and transient Cre expression, cells were electroporated with the following constructs: (*i*) R1 ES cells with 20 μg of pM2TV linearized with *Not*I, followed by G418 selection to obtain the *M2* allele; (*ii*) *M2*/+ cells with 15 μg of circular pBS165, a PGK-Cre expression vector (55) to obtain the *M2loxP* allele; (*iii*) *M2loxP*/+ cells with 20 μg of pI2TV linearized with *Not*I (30), followed by G418 selection to obtain the *I2* allele; (*iv*) *M2loxP*/+ *I2*/+ or simply *I2*/+ cells with 15 μg of circular pCAGGS-nlsCre, a subclone of nlsCre into pCAGGS ((56); A.N.) to obtain cells carrying the deletion allele or *I2loxP*.

## Mice and ES cell lines

R1 ES cell clones targeted at *Ascl2*, *Ins2*, or carrying the deletion allele, were aggregated with diploid host embryos as described (54). Mutant mice carrying the *lox*P site insertion alleles on Chr 7 were maintained on an outbred background (ICR, Harlan). The *Sycp1-Cre* transgenic mice (35) were obtained from Dr. F. Cuzin (Nice). *Mus musculus castaneus* mice were from the Jackson Laboratories (CAST/EiJ strain). The congenic mouse line with distal Chr 7 *M. m. castaneus* SNPs on the 129S1 background was derived in our laboratory (129S1cCAST7/Lef). For all the genotypes of ES cells and mice described here, the maternally inherited allele is always presented first. The nomenclature for the new TAMERE alleles are Del(7*Ascl2-Ins2*)1Lef (synonym $Del^{7AI}$) for the deletion and *Dp*(7*Ascl2-Ins2*)1Lef (synonym $Dp^{7AI}$) for the duplication allele.

## Genotyping

The nucleotide sequences for all primers used in this study are given in the Supplementary Table 1. The segregation of the *Sycp1-Cre* transgene was monitored using a PCR-based Cre-

specific genotyping with the PCR oligos MCKCre5′ and MCKCre3′ and annealing at 50°C. *M2* to *M2loxP* excision from *Sycp1-Cre* transgenic males was detected by PCR amplification from the *PGK* promoter (forward primer PGK2) to downstream *Ascl2* sequences (reverse primer MR1). PCR products of 1.3 kb (*M2loxP*) and 2.5 kb (*M2*) are obtained using the long-range Expand Taq (Roche) on purified genomic DNA samples from tails or ES cells. Analysis of the TAMERE products used the PCR primers F1, R1, F2, and R2 (Fig. 2B). In the duplication allele $Dp^{7AI}$, a new junction generated between the 5′ of *Ins2* and the 3′ end of *Ascl2* is detected by a highly specific PCR reaction using the primers F2 and R1 (*Taq*, annealing at 60°C, 225-bp product). The PCR genotyping of $Del^{7AI}$ on tail genomic DNA from TAMERE (Fig. 3C) is based on the detection of a new *Ascl2-neo* junction by Expand *Taq* amplification with primers F1 and R2 (840 bp). For genotyping of $Del^{7AI}$ mice, we simply amplified the *Ascl2-PGK* junction (the Δ5′ PCR reaction), as described (30). Homozygous mutant embryos were detected by a positive Δ5′ PCR reaction and absence of a wild-type band for a PCR reaction spanning the *I2* allele (I2wt reaction).

Two SNP detection assays based on genomic PCR and RFLP were used in the experiments involving the CAST mice. The assay for the SNP within exon 3 of *Ascl2* has been described (30). A 511-bp PCR product from intron 2 to exon 3 (primers in2F1 and 726R) was digested with *Hpa*II to yield fragments of 217, 198 and 96 bp for *M. m. musculus* alleles instead of 313 and 198 bp for CAST. The *Ascl2* 3′ flanking SNP, internal to the deletion was assayed by Expand *Taq* amplification with primers M2F and MR1 and digestion of the 618-bp product with *Xba*I, which cut only the CAST allele (468 and 150 bp bands).

## DNA FISH

Three PAC clones from the RPCI-21 (129S6) mouse genomic DNA library and spanning the distal Chr 7 domain were used for DNA FISH experiments: the clones span the loci *H19* (29G9), *Th* (231E13), and *Phlda2* (210N7) (57). PAC DNA was purified using the Large-Construct kit (Qiagen) and directly labeled with fluorescein isothiocyanate (*H19*, *Phlda2*) or Texas Red (*Th*) by nick translation (Vysis, Downers Grove, IL). Metaphase spreads were obtained from primary embryonic fibroblasts derived from E14.5 embryos heterozygous for the $Del^{7AI}$ allele (+/$Del^{7AI}$ genotype) or their wild-type littermate. Images were acquired and analyzed with an SD 200 Spectral Bio-imaging System (ASI Ltd., MigdalHaemek, Israel) attached to a Zeiss Axioplan 2 microscope (Carl Zeiss, Canada).

## RNA purification and analysis

For the analysis of imprinted expression of the *H19* and *Kcnq1ot1* ncRNA, conceptuses from reciprocal crosses between CAST/Ei (or 129S1cCAST7/Lef) mice and +/$Del^{7AI}$ heterozygotes were recovered at E13.5 as described (54). Embryonic RNA was purified using Trizol (Invitrogen) and processed for RT-PCR by random priming using the reverse transcriptase SuperScript II (Invitrogen) on DNase-treated RNA (RQ1, Promega). The allele-specific *H19* analysis was based on a polymorphic *Cac*8I site present in the *castaneus* RT-PCR product (58). The 641-bp PCR products were digested with *Bts*XI and *Cac*8I to yield bands of 418 and 223 bp for the *domesticus* allele but 277, 223 and 131 for castaneus. The expressed *Kcnq1ot1 Stu*I polymorphism was kindly provided by Melissa Mann. The 465-bp PCR products were digested with *Ssp*I and *Stu*I. The bands are of 402 and 63 bp for

*domesticus,* 252, 150 and 63 bp for *castaneus.* All primer sequences are in Table S3 of the Supplementary Material.

### DNA bisulfite modification and sequencing

Genomic DNA samples isolated from reciprocal CAST/DelTel7 and DelTel7/CAST E9.5 embryos were subjected to bisulfite modification, PCR amplification, subcloning, and sequencing as described (9). For IC1 (H19 DMR, Fig. 5A), nested PCR reactions encompassing known domesticus/castaneus SNPs were carried out as described previously (but see TABLE 1 for primer modifications), with primers BMsp2t1 + BHha1t3, followed by BMsp2t2.2 + BHha2t4.2; note that these two primers were modified from the published sequence to reflect correction with the current genomic sequence of IC1 in our strains (59). For IC2 (KvDMR1, Fig. 6D), the assays were performed as described (4), except that we did not use the outer forward primer Kcnq1ot1 OF since it overlaps with a CpG. We used a semi-nested approach, with primers Kcnq1ot1 IF + Kcnq1ot1 OR followed by Kcnq1ot1 IF + Kcnq1ot1 IR (4). The parental alleles are distinguished by an A50C transversion, identified by sequencing CAST genomic DNA (*dom* A50 / *cast* C50). PCR products were cloned into pGEM-T vector (Promega) and transformed into TOP10 cells (Invitrogen). Primer sequences are available in Table S3 of the Supplementary Material. For each DNA sample, we performed two independent bisulfite treatments; each bisulfite-treated DNA was amplified in two independent PCR reactions. We sequenced 3 to 5 cloned stands per PCR reaction and analyzed the data using BiQ Analyzer (60).

## Supplementary Material

Refer to Web version on PubMed Central for supplementary material.

## Acknowledgments

We thank Jeff Mann and Mellissa Mann for information on the *Ascl2* and *Kcnq1ot1 M. m. castaneus* polymorphism, respectively, Michael Higgins for providing the Chr 7 PAC clones, and François Cuzin for kindly providing the *Sycp1*-Cre transgenic mice.

**Funding**

This work was supported in part by the Canadian Institutes of Health Research (MOP-82863 to L.L. and FRN 13687 to A.N.). L.L. holds a Canada Research Chair and was also supported by a Michael Smith Foundation for Health Research (MSFHR) Scholar Award.

## References

1. Verona R, Mann MR, Bartolomei M. Genomic imprinting: intricacies of epigenetic regulation in clusters. Annu Rev Cell Dev Biol. 2003; 19:237–259. [PubMed: 14570570]
2. Maher ER, Reik W. Beckwith-Wiedemann syndrome: imprinting in clusters revisited. J Clin Invest. 2000; 105:247–252. [PubMed: 10675349]
3. Weksberg R, Smith AC, Squire J, Sadowski P. Beckwith-Wiedemann syndrome demonstrates a role for epigenetic control of normal development. Hum Mol Genet. 2003; 12(Spec No 1):R61–8. [PubMed: 12668598]
4. Engemann S, Strödicke M, Paulsen M, Franck O, Reinhardt R, Lane N, Reik W, Walter J. Sequence and functional comparison in the Beckwith-Wiedemann region: implications for a novel imprinting centre and extended imprinting. Hum Mol Genet. 2000; 9:2691–2706. [PubMed: 11063728]

5. Onyango P, Miller W, Lehoczky J, Leung CT, Birren B, Wheelan S, Dewar K, Feinberg A. Sequence and comparative analysis of the mouse 1-megabase region orthologous to the human 11p15 imprinted domain. Genome Res. 2000; 10:1697–1710. [PubMed: 11076855]
6. Paulsen M, El-Maarri O, Engemann S, Strödicke M, Franck O, Davies K, Reinhardt R, Reik W, Walter J. Sequence conservation and variability of imprinting in the Beckwith-Wiedemann syndrome gene cluster in human and mouse. Hum Mol Genet. 2000; 9:1829–1841. [PubMed: 10915772]
7. Bartolomei M, Webber A, Brunkow M, Tilghman S. Epigenetic mechanisms underlying the imprinting of the mouse H19 gene. Genes Dev. 1993; 7:1663–1673. [PubMed: 7690336]
8. Ferguson-Smith AC, Sasaki H, Cattanach BM, Surani MA. Parental-origin-specific epigenetic modification of the mouse H19 gene. Nature. 1993; 362:751–755. [PubMed: 8469285]
9. Tremblay KD, Saam JR, Ingram RS, Tilghman S, Bartolomei M. A paternal-specific methylation imprint marks the alleles of the mouse H19 gene. Nat Genet. 1995; 9:407–413. [PubMed: 7795647]
10. Thorvaldsen JL, Duran KL, Bartolomei M. Deletion of the H19 differentially methylated domain results in loss of imprinted expression of H19 and Igf2. Genes Dev. 1998; 12:3693–3702. [PubMed: 9851976]
11. Bell AC, Felsenfeld G. Methylation of a CTCF-dependent boundary controls imprinted expression of the Igf2 gene. Nature. 2000; 405:482–485. [PubMed: 10839546]
12. Hark AT, Schoenherr CJ, Katz DJ, Ingram RS, Levorse JM, Tilghman S. CTCF mediates methylation-sensitive enhancer-blocking activity at the H19/Igf2 locus. Nature. 2000; 405:486–489. [PubMed: 10839547]
13. Srivastava M, Hsieh S, Grinberg A, Williams-Simons L, Huang SP, Pfeifer K. H19 and Igf2 monoallelic expression is regulated in two distinct ways by a shared cis acting regulatory region upstream of H19. Genes Dev. 2000; 14:1186–1195. [PubMed: 10817754]
14. Szabó P, Tang SH, Rentsendorj A, Pfeifer GP, Mann JR. Maternal-specific footprints at putative CTCF sites in the H19 imprinting control region give evidence for insulator function. Curr Biol. 2000; 10:607–610. [PubMed: 10837224]
15. Lee MP, DeBaun MR, Mitsuya K, Galonek HL, Brandenburg S, Oshimura M, Feinberg A. Loss of imprinting of a paternally expressed transcript, with antisense orientation to KVLQT1, occurs frequently in Beckwith-Wiedemann syndrome and is independent of insulin-like growth factor II imprinting. Proc Natl Acad Sci USA. 1999; 96:5203–5208. [PubMed: 10220444]
16. Smilinich NJ, Day CD, Fitzpatrick GV, Caldwell GM, Lossie AC, Cooper PR, Smallwood AC, Joyce JA, Schofield PN, Reik W, Nicholls RD, Weksberg R, Driscoll DJ, Maher ER, Shows TB, Higgins MJ. A maternally methylated CpG island in KvLQT1 is associated with an antisense paternal transcript and loss of imprinting in Beckwith-Wiedemann syndrome. Proc Natl Acad Sci USA. 1999; 96:8064–8069. [PubMed: 10393948]
17. Fitzpatrick G, Soloway P, Higgins M. Regional loss of imprinting and growth deficiency in mice with a targeted deletion of KvDMR1. Nat Genet. 2002; 32:426–431. [PubMed: 12410230]
18. Ainscough JF, Koide T, Tada M, Barton S, Surani MA. Imprinting of Igf2 and H19 from a 130 kb YAC transgene. Development. 1997; 124:3621–3632. [PubMed: 9342054]
19. Cerrato F, Sparago A, Di Matteo I, Zou X, Dean W, Sasaki H, Smith P, Genesio R, Bruggemann M, Reik W, Riccio A. The two-domain hypothesis in Beckwith-Wiedemann syndrome: autonomous imprinting of the telomeric domain of the distal chromosome 7 cluster. Hum Mol Genet. 2005; 14:503–511. [PubMed: 15640248]
20. Giddings SJ, King CD, Harman KW, Flood JF, Carnaghi LR. Allele specific inactivation of insulin 1 and 2, in the mouse yolk sac, indicates imprinting. Nat Genet. 1994; 6:310–313. [PubMed: 8012396]
21. Guillemot F, Caspary T, Tilghman S, Copeland NG, Gilbert DJ, Jenkins NA, Anderson DJ, Joyner AL, Rossant J, Nagy A. Genomic imprinting of Mash2, a mouse gene required for trophoblast development. Nat Genet. 1995; 9:235–242. [PubMed: 7773285]
22. Patton SJ, Luke GN, Holland PW. Complex history of a chromosomal paralogy region: insights from amphioxus aromatic amino acid hydroxylase genes and insulin-related genes. Mol Biol Evol. 1998; 15:1373–1380. [PubMed: 12572601]

23. Paulsen M, Khare T, Burgard C, Tierling S, Walter J. Evolution of the Beckwith-Wiedemann syndrome region in vertebrates. Genome Res. 2005; 15:146–153. [PubMed: 15590939]
24. Giannoukakis N, Deal C, Paquette J, Goodyer CG, Polychronakos C. Parental genomic imprinting of the human IGF2 gene. Nat Genet. 1993; 4:98–101. [PubMed: 8099843]
25. Moore GE, Abu-Amero SN, Bell G, Wakeling EL, Kingsnorth A, Stanier P, Jauniaux E, Bennett ST. Evidence that insulin is imprinted in the human yolk sac. Diabetes. 2001; 50:199–203. [PubMed: 11147788]
26. Ohlsson R, Nyström A, Pfeifer-Ohlsson S, Töhönen V, Hedborg F, Schofield P, Flam F, Ekström TJ. IGF2 is parentally imprinted during human embryogenesis and in the Beckwith-Wiedemann syndrome. Nat Genet. 1993; 4:94–97. [PubMed: 8513333]
27. Schulz R, Menheniott TR, Woodfine K, Wood A, Choi J, Oakey R. Chromosome-wide identification of novel imprinted genes using microarrays and uniparental disomies. Nucleic Acids Res. 2006; 34:e88. [PubMed: 16855283]
28. Shirohzu H, Yokomine T, Sato C, Kato R, Toyoda A, Purbowasito W, Suda C, Mukai T, Hattori M, Okumura K, Sakaki Y, Sasaki H. A 210-kb segment of tandem repeats and retroelements located between imprinted subdomains of mouse distal chromosome 7. DNA Res. 2004; 11:325–334. [PubMed: 15747580]
29. Zhao Z, Tavoosidana G, Sjölinder M, Göndör A, Mariano P, Wang S, Kanduri C, Lezcano M, Sandhu KS, Singh U, Pant V, Tiwari V, Kurukuti S, Ohlsson R. Circular chromosome conformation capture (4C) uncovers extensive networks of epigenetically regulated intra- and interchromosomal interactions. Nat Genet. 2006; 38:1341–1347. [PubMed: 17033624]
30. Oh R, Ho R, Mar L, Gertsenstein M, Paderova J, Hsien J, Squire JA, Higgins M, Nagy A, Lefebvre L. Epigenetic and phenotypic consequences of a truncation disrupting the imprinted domain on distal mouse chromosome 7. Mol Cell Biol. 2008; 28:1092–1103. [PubMed: 18039841]
31. Nagy A, Rossant J, Nagy R, Abramow-Newerly W, Roder JC. Derivation of completely cell culture-derived mice from early-passage embryonic stem cells. Proc Natl Acad Sci USA. 1993; 90:8424–8428. [PubMed: 8378314]
32. Hérault Y, Rassoulzadegan M, Cuzin F, Duboule D. Engineering chromosomes in mice through targeted meiotic recombination (TAMERE). Nat Genet. 1998; 20:381–384. [PubMed: 9843213]
33. Tarchini B, Huynh TH, Cox GA, Duboule D. HoxD cluster scanning deletions identify multiple defects leading to paralysis in the mouse mutant Ironside. Genes Dev. 2005; 19:2862–2876. [PubMed: 16322559]
34. Chung SS, Cuzin F, Rassoulzadegan M, Wolgemuth DJ. Primary spermatocyte-specific Cre recombinase activity in transgenic mice. Transgenic Res. 2004; 13:289–294. [PubMed: 15359605]
35. Vidal F, Sage J, Cuzin F, Rassoulzadegan M. Cre expression in primary spermatocytes: a tool for genetic engineering of the germ line. Mol Reprod Dev. 1998; 51:274–280. [PubMed: 9771647]
36. Constância M, Hemberger M, Hughes J, Dean W, Ferguson-Smith A, Fundele R, Stewart F, Kelsey G, Fowden A, Sibley C, Reik W. Placental-specific IGF-II is a major modulator of placental and fetal growth. Nature. 2002; 417:945–948. [PubMed: 12087403]
37. DeChiara TM, Robertson EJ, Efstratiadis A. Parental imprinting of the mouse insulin-like growth factor II gene. Cell. 1991; 64:849–859. [PubMed: 1997210]
38. Hatada I, Mukai T. Genomic imprinting of p57KIP2, a cyclin-dependent kinase inhibitor, in mouse. Nat Genet. 1995; 11:204–206. [PubMed: 7550351]
39. Yan Y, Frisén J, Lee M, Massagué J, Barbacid M. Ablation of the CDK inhibitor p57Kip2 results in increased apoptosis and delayed differentiation during mouse development. Genes Dev. 1997; 11:973–983. [PubMed: 9136926]
40. Zhang P, Liégeois NJ, Wong C, Finegold M, Hou H, Thompson JC, Silverman A, Harper JW, DePinho RA, Elledge SJ. Altered cell differentiation and proliferation in mice lacking p57KIP2 indicates a role in Beckwith-Wiedemann syndrome. Nature. 1997; 387:151–158. [PubMed: 9144284]
41. Frank D, Fortino W, Clark L, Musalo R, Wang W, Saxena A, Li CM, Reik W, Ludwig T, Tycko B. Placental overgrowth in mice lacking the imprinted gene Ipl. Proc Natl Acad Sci USA. 2002; 99:7490–7495. [PubMed: 12032310]

42. Guillemot F, Nagy A, Auerbach A, Rossant J, Joyner AL. Essential role of Mash-2 in extraembryonic development. Nature. 1994; 371:333–336. [PubMed: 8090202]
43. Kobayashi K, Morita S, Sawada H, Mizuguchi T, Yamada K, Nagatsu I, Hata T, Watanabe Y, Fujita K, Nagatsu T. Targeted disruption of the tyrosine hydroxylase locus results in severe catecholamine depletion and perinatal lethality in mice. J Biol Chem. 1995; 270:27235–27243. [PubMed: 7592982]
44. Zhou QY, Quaife CJ, Palmiter RD. Targeted disruption of the tyrosine hydroxylase gene reveals that catecholamines are required for mouse fetal development. Nature. 1995; 374:640–643. [PubMed: 7715703]
45. Ager EI, Pask A, Gehring HM, Shaw G, Renfree M. Evolution of the CDKN1C-KCNQ1 imprinted domain. BMC Evol Biol. 2008; 8:163. [PubMed: 18510768]
46. Paulsen M, Davies KR, Bowden LM, Villar AJ, Franck O, Fuermann M, Dean WL, Moore TF, Rodrigues N, Davies KE, Hu RJ, Feinberg A, Maher ER, Reik W, Walter J. Syntenic organization of the mouse distal chromosome 7 imprinting cluster and the Beckwith-Wiedemann syndrome region in chromosome 11p15.5. Hum Mol Genet. 1998; 7:1149–1159. [PubMed: 9618174]
47. Yokomine T. Structural and functional analysis of a 0.5-Mb chicken region orthologous to the imprinted mammalian Ascl2/Mash2-Igf2-H19 region. Genome Res. 2005; 15:154–165. [PubMed: 15590938]
48. Duvillié B, Bucchini D, Tang T, Jami J, Pàldi A. Imprinting at the mouse Ins2 locus: evidence for cis- and trans-allelic interactions. Genomics. 1998; 47:52–57. [PubMed: 9465295]
49. Duvillié B, Cordonnier N, Deltour L, Dandoy-Dron F, Itier JM, Monthioux E, Jami J, Joshi RL, Bucchini D. Phenotypic alterations in insulin-deficient mutant mice. Proc Natl Acad Sci USA. 1997; 94:5137–5140. [PubMed: 9144203]
50. Leroux L, Desbois P, Lamotte L, Duvillié B, Cordonnier N, Jackerott M, Jami J, Bucchini D, Joshi RL. Compensatory responses in mice carrying a null mutation for Ins1 or Ins2. Diabetes. 2001; 50(Suppl 1):S150–3. [PubMed: 11272179]
51. Lüdecke B, Dworniczak B, Bartholomé K. A point mutation in the tyrosine hydroxylase gene associated with Segawa's syndrome. Hum Genet. 1995; 95:123–125. [PubMed: 7814018]
52. Andrews S, Wood M, Tunster S, Barton S, Surani M, John R. Cdkn1c (p57Kip2) is the major regulator of embryonic growth within its imprinted domain on mouse distal chromosome 7. BMC Dev Biol. 2007; 7:53. [PubMed: 17517131]
53. John RM, Ainscough JF, Barton SC, Surani MA. Distant cis-elements regulate imprinted expression of the mouse p57(Kip2) (Cdkn1c) gene: implications for the human disorder, Beckwith--Wiedemann syndrome. Hum Mol Genet. 2001; 10:1601–1609. [PubMed: 11468278]
54. Nagy, A., Gertsenstein, M., Vintersten, K., Behringer, R. Manipulating the mouse embryo: a laboratory manual. Cold Spring Harbor Laboratory Press; 2003.
55. Sauer B. Manipulation of transgenes by site-specific recombination: use of Cre recombinase. Methods Enzymol. 1993; 225:890–900. [PubMed: 8231893]
56. Niwa H, Yamamura K, Miyazaki J. Efficient selection for high-expression transfectants with a novel eukaryotic vector. Gene. 1991; 108:193–199. [PubMed: 1660837]
57. Day CD, Smilinich NJ, Fitzpatrick GV, deJong PJ, Shows TB, Higgins MJ. The imprinted domain in mouse distal Chromosome 7: reagents for mutagenesis and sequencing. Mamm Genome. 1999; 10:182–185. [PubMed: 9922400]
58. Thorvaldsen JL, Mann MR, Nwoko O, Duran KL, Bartolomei M. Analysis of sequence upstream of the endogenous H19 gene reveals elements both essential and dispensable for imprinting. Mol Cell Biol. 2002; 22:2450–2462. [PubMed: 11909940]
59. Davis TL, Trasler JM, Moss SB, Yang GJ, Bartolomei M. Acquisition of the H19 methylation imprint occurs differentially on the parental alleles during spermatogenesis. Genomics. 1999; 58:18–28. [PubMed: 10331941]
60. Bock C. BiQ Analyzer: visualization and quality control for DNA methylation data from bisulfite sequencing. Bioinformatics. 2005; 21:4067–4068. [PubMed: 16141249]

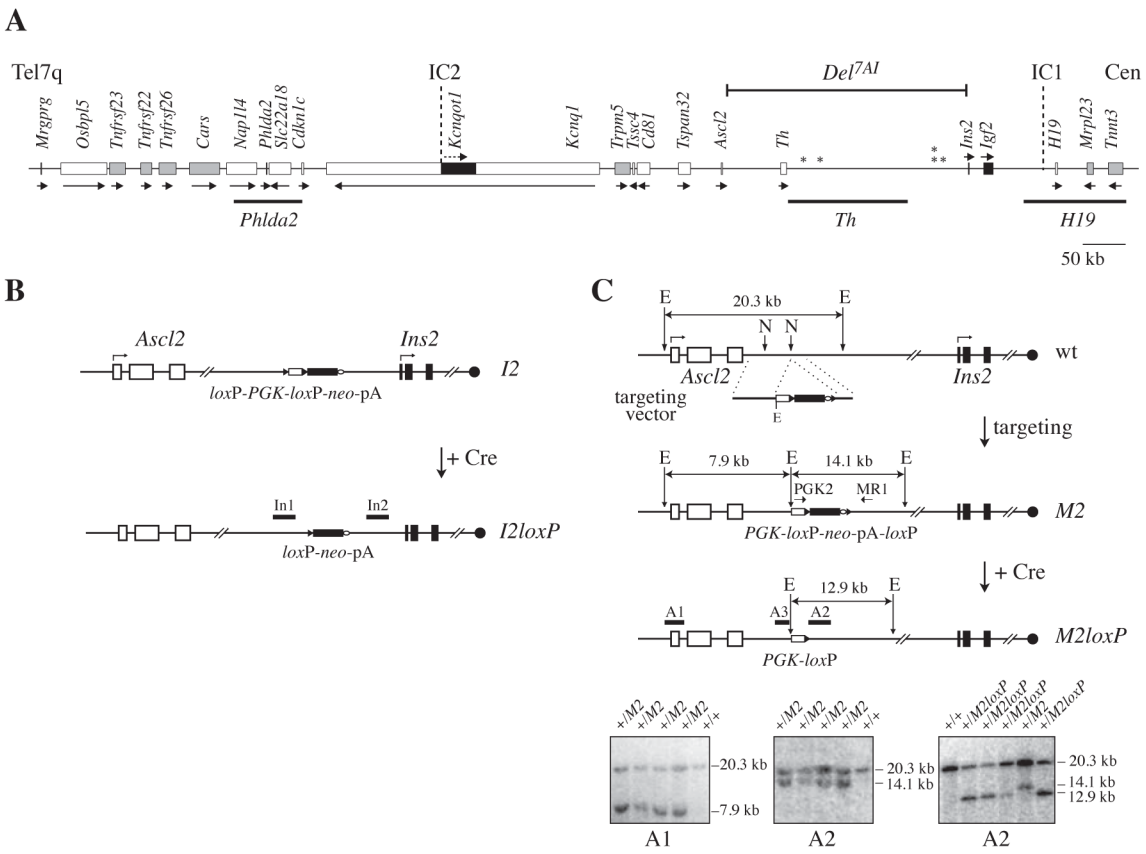


**Figure 1. Targeted *lox*P site insertions on distal Chr7**

(**A**) Gene arrangement on distal Chr 7 shown to scale (coordinates from NCBI m37 build), oriented from the telomere (Tel7q, left) to the centromere (Cen, right). Genes showing biallelic, paternal and maternal expressions are represented by shaded, black, and white rectangles, respectively, with arrows indicating their transcriptional orientation. The map also presents the positions of the following features: (above) the imprinting centers IC1 and IC2, the sites physically interacting with the maternal IC1 (asterisks) and the breakpoints of the deletion generated in this study (*Del*$^{7AI}$); (below) three genomic PAC clones (*Phlda2*, *Th*, and *H19*) used in DNA FISH experiments. (**B**) Targeting of a *lox*P site at *Ins2*: the *I2* and *I2loxP* alleles. The generation of these alleles has been described previously (30). White and black rectangles show the *Ascl2* and *Ins2* exons, respectively. The black circle on the right represents the centromere. In the *I2* allele, the *PGK* promoter can be deleted by Cre. The remaining promoter-less *lox*P-*neo*-pA of the *I2loxP* allele can be activated by recombination with the *PGK*-*lox*P of the *M2loxP* allele, shown in C. The genomic probe In1 was used to analyze the duplication allele (Supplementary Fig. S3); In2 was used to confirm the structure of the deletion allele (Fig. 3A). (**C**) Targeting of a *lox*P site at *Ascl2*: the *M2* and *M2loxP* alleles. Diagrams centered on the *Ascl2*-*Ins2* interval and showing, from the top, the wild-type locus (wt), the targeting vector, the targeted *M2* allele and the *M2loxP* insertion. The selectable marker cassettes consist of a *PGK* promoter (white box), driving *neo* expression from a *neo*-pA construct (black box and open oval). In the *M2* allele the *neo*-pA is flanked by *lox*P sites (black arrowheads). A1: external 5′ probe; A2, A3: 3′ and 5′

internal genomic probes. E, *Eco*RI; N, *Nco*I. Southern blot analysis of genomic DNA from ES cell clones, digested with *Eco*RI and hybridized with A1 and A2 (bottom left and middle). The *M2loxP* allele was obtained by transient Cre expression in $Ascl2^{+/M2}$ cells and analyzed with probe A2 (bottom right). Samples include the parental R1 ES cell line (+/+), 4 positive $Ascl2^{+/M2loxP}$ and one un-recombined $Ascl2^{+/M2}$ clones. PGK2 and MR1 on *M2* allele: PCR primers used to genotype the *M2* and *M2loxP* alleles (Supplementary Fig. S2B). The A3 probe was used to monitor rearrangements at the *M2* allele *in vivo* (Fig. S2A), and to confirm the structure of the deletion allele (Fig. 3A).

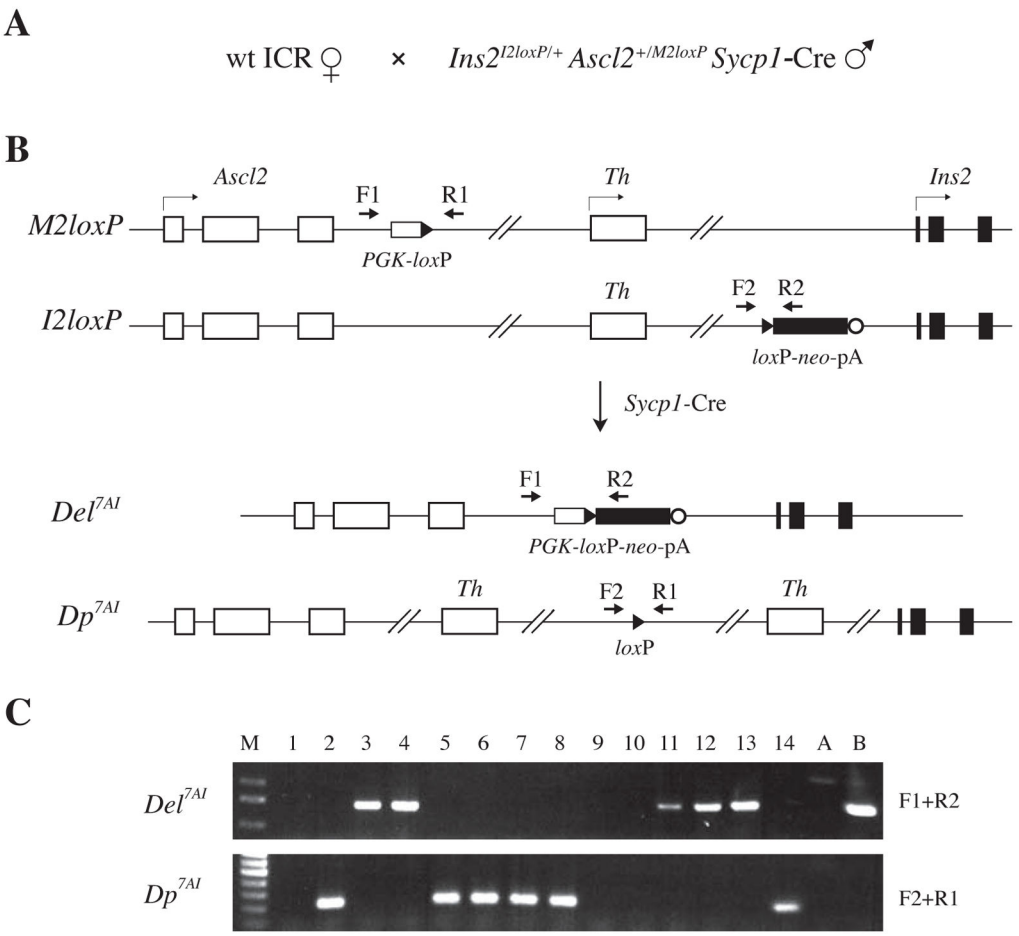


**Figure 2. TAMERE from a triple transgenic male: the *Del*$^{7AI}$ and *Dp*$^{7AI}$ alleles**

(**A**) Breeding scheme to produce novel recombined alleles from wild-type females crossed with triple transgenic males, carrying the *Sycp1*-Cre transgene as well as *lox*P site insertions at the maternal *Ins2* and paternal *Ascl2* loci. (**B**) Diagrams of the *Ascl2-Ins2* interval presented as in Fig. 1 and showing the positions of the genotyping PCR primers F1, F2, R1, and R2. From the top, these show the structures of the *lox*P insertion alleles at *Ascl2* (*M2loxP*) and *Ins2* (*I2loxP*) present in the male, as well as the two predicted reciprocal recombination products from a *trans*-allelic Cre reaction: the deletion allele *Del*$^{7AI}$ and the duplication allele *Dp*$^{7AI}$. (**C**) Representative PCR genotyping of 14 progeny, including 5 +/*Del*$^{7AI}$ heterozygotes (#3, 4, 11–13) and 6 +/*Dp*$^{7AI}$ heterozygotes (#2, 5–8, 14). The new alleles were detected using specific PCR assays against novel unique junctions. Controls are: A, wild-type DNA; B, ES cells heterozygous for the deletion allele.

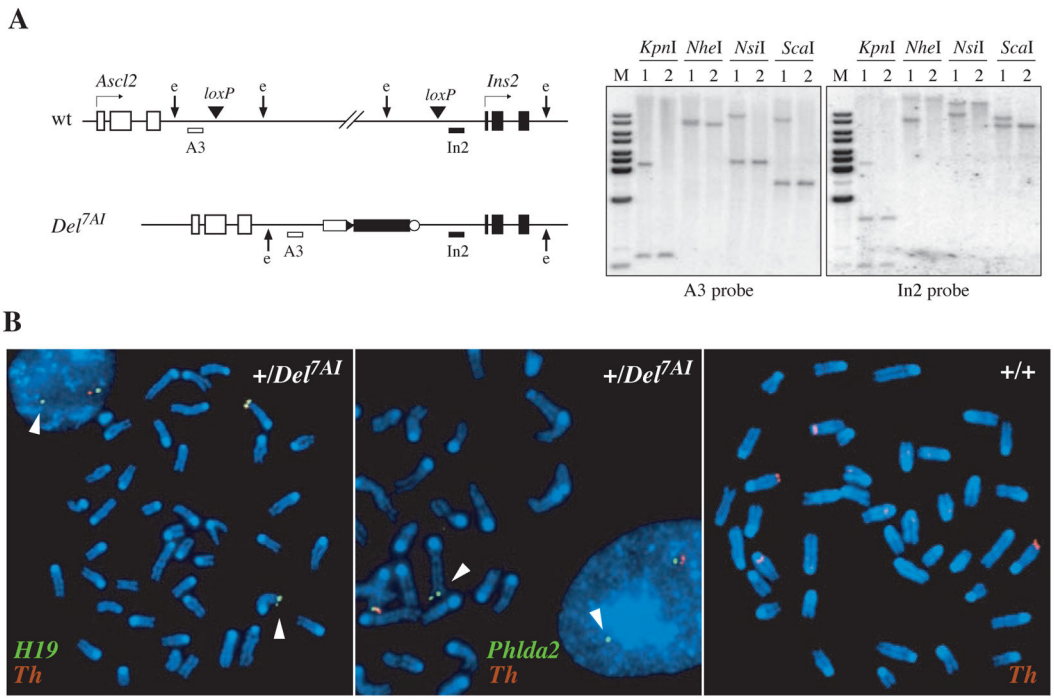


**Figure 3. Molecular and cytogenetic characterization of the deletion allele *Del*$^{7AI}$**

(**A**) Southern blot analysis of tail genomic DNA, isolated from a +/*Del*$^{7AI}$ heterozygote (#1) and a wild-type littermate (#2), digested with different restriction enzymes, and probed with the *Ascl2* and *Ins2* genomic probes A3 and In2. The diagrams of the wild-type (wt) and mutant (*Del*$^{7AI}$) alleles (left) present the positions of the probes A3 and In2 relative to the *lox*P site insertion sites. Representative restriction enzyme recognition sites (e) illustrate the presence of a new fragment shared by the two probes in the DNA sample from the +/*Del*$^{7AI}$ heterozygote (#1). **(B)** DNA FISH on interphase nuclei and metaphase chromosome spreads from wild-type or +/*Del*$^{7AI}$ primary embryonic fibroblasts, using genomic PAC clones from Chr 7 regions proximal (*H19*, green), internal (*Th*, red), or distal (*Phlda2,* green) to the *Del*$^{7AI}$ breakpoints as probes (Fig. 1A). Arrowheads point to Chr 7 variants negative for the *Th* probe and thus carrying the *Del*$^{7AI}$ allele.

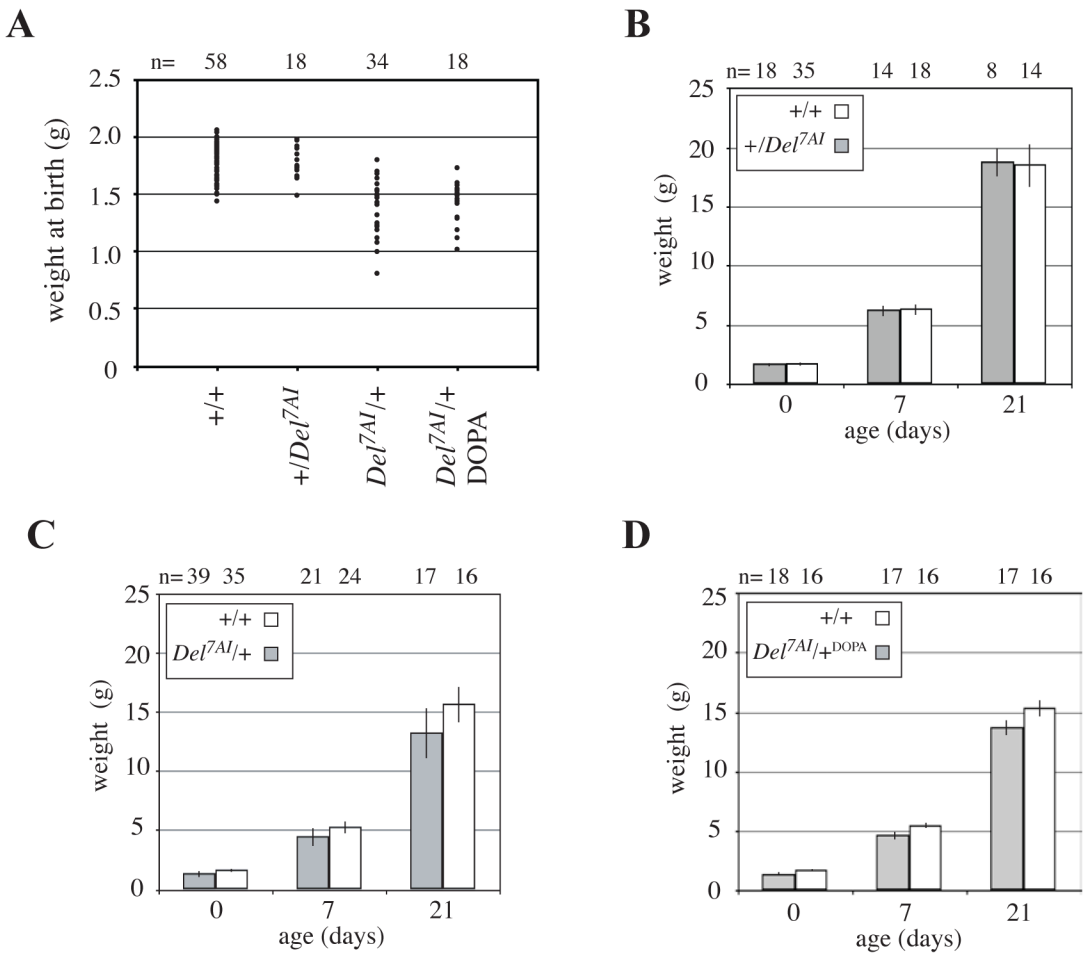


**Figure 4. Intrauterine growth restriction in maternal *Del*$^{7AI}$ heterozygotes**

Newborns from five litters obtained by crossing +/*Del*$^{7AI}$ heterozygous females to wild type CD-1 outbred males and from six reciprocal crosses were weighted the morning of their delivery (p0) and genotyped. (**A**) Scatter plot showing the distribution of the weights at birth. The average weight of maternal heterozygous pups (1.42g) is 17.4% smaller than that of their wild-type litter mates (1.72g). Between the maternal heterozygotes and wild-type pups, p=1.82E-8 (*t*-Test). Number of animals analyzed: n=58 wild-type, n=18 +/*Del*$^{7AI}$, n=34 *Del*$^{7AI}$/+, and n=18 +/*Del*$^{7AI}$ treated with L-DOPA. (**B**) to (**D**) Body weight of mutant and wild-type litter mates at p0, p7 and p21 (time of weaning). Unlike the paternal heterozygotes (+/*Del*$^{7AI}$), maternal heterozygous pups (*Del*$^{7AI}$/+) do not catch up to their wild-type litter mates before weaning. This growth retardation is not rescue by addition of L-DOPA to the drinking water of pregnant females. Bars show the average weight ± standard deviation. At each time point, p<0.001 (*t*-Test) between maternal heterozygotes and wild-types in C. All values and numbers of animals analyzed are given in Table S2, in the Supplementary Material.

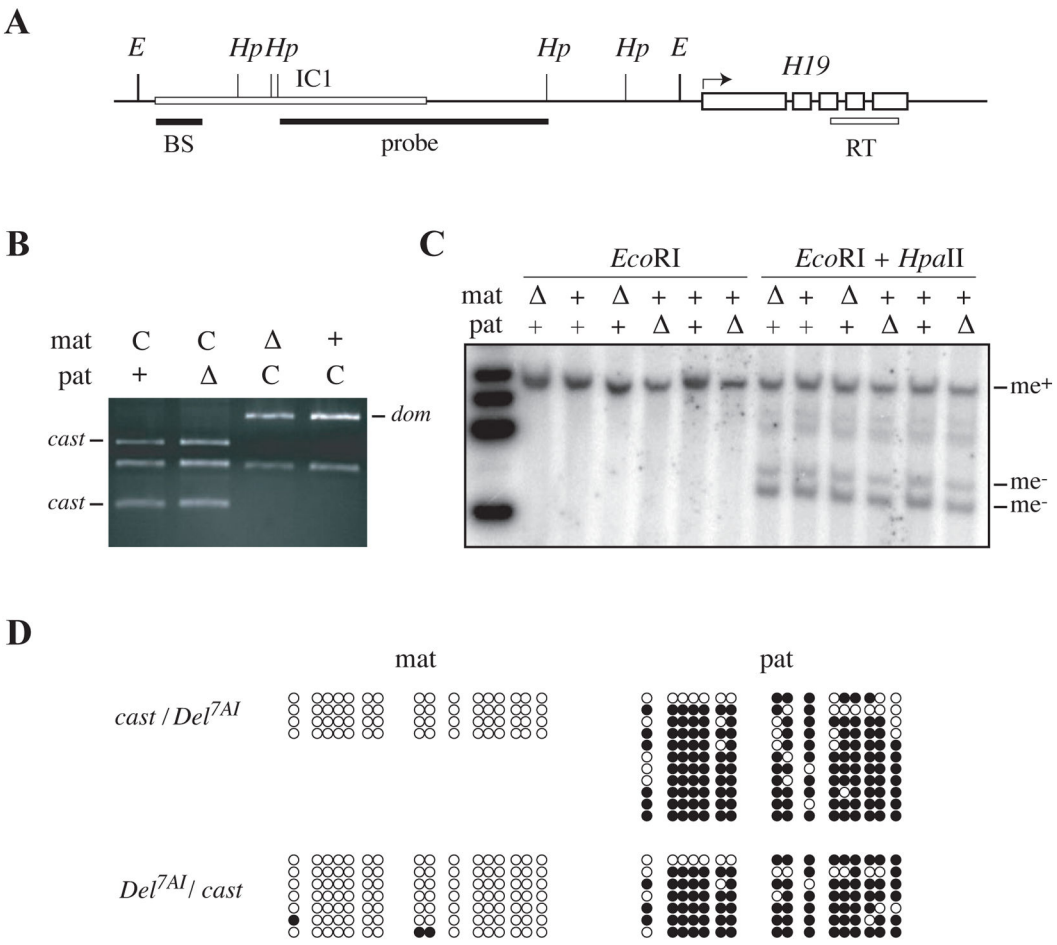


**Figure 5. Maintenance of imprinting at IC1 in reciprocal *Del*$^{7AI}$ heterozygotes**

Expression and methylation imprinting at IC1 were analyzed in reciprocal heterozygotes for the *Del*$^{7AI}$ allele. E14.5 embryos were recovered from reciprocal crosses between +/*Del*$^{7AI}$ heterozygotes and *M.m.castaneus* (CAST/EiJ) adult mice. (**A**) Diagram of the IC1-*H19* region showing the region amplified by RT-PCR to analyze *H19* expression in B (RT), the position of the genomic probe used in C (probe) and the part of IC1 analyzed in D (BS). (**B**) Allele-specific RT-PCR analysis of embryonic *H19* expression. Maternal (mat) and paternal (pat) alleles are as follows: C, wild-type *castaneus*; +, wild-type *domesticus*; and Δ, *Del*$^{7AI}$. A *Cac*8I RFLP was used to distinguish the *castaneus* (*cast*) from the *domesticus* (*dom*) variants. (**C**) DNA methylation analysis by Southern blotting of genomic DNA digested with *Eco*RI (*E*) and the methylation sensitive restriction enzyme *Hpa*II (*Hp*). Maternal (mat) and paternal (pat) alleles are identified as wild-type (+) or *Del*$^{7AI}$ (Δ). Also shown are the positions of methylated *Eco*RI fragment (me+) and the main unmethylated (me-) bands. (**D**) Allele-specific DNA methylation analysis by sodium bisulfite sequencing. The upstream region of the IC1 DMR was analyzed in reciprocal *Del*$^{7AI}$ heterozygotes carrying SNPs allowing the identification of the parental alleles. Methylated CpG sites are shown in black, unmethylated sites in white.

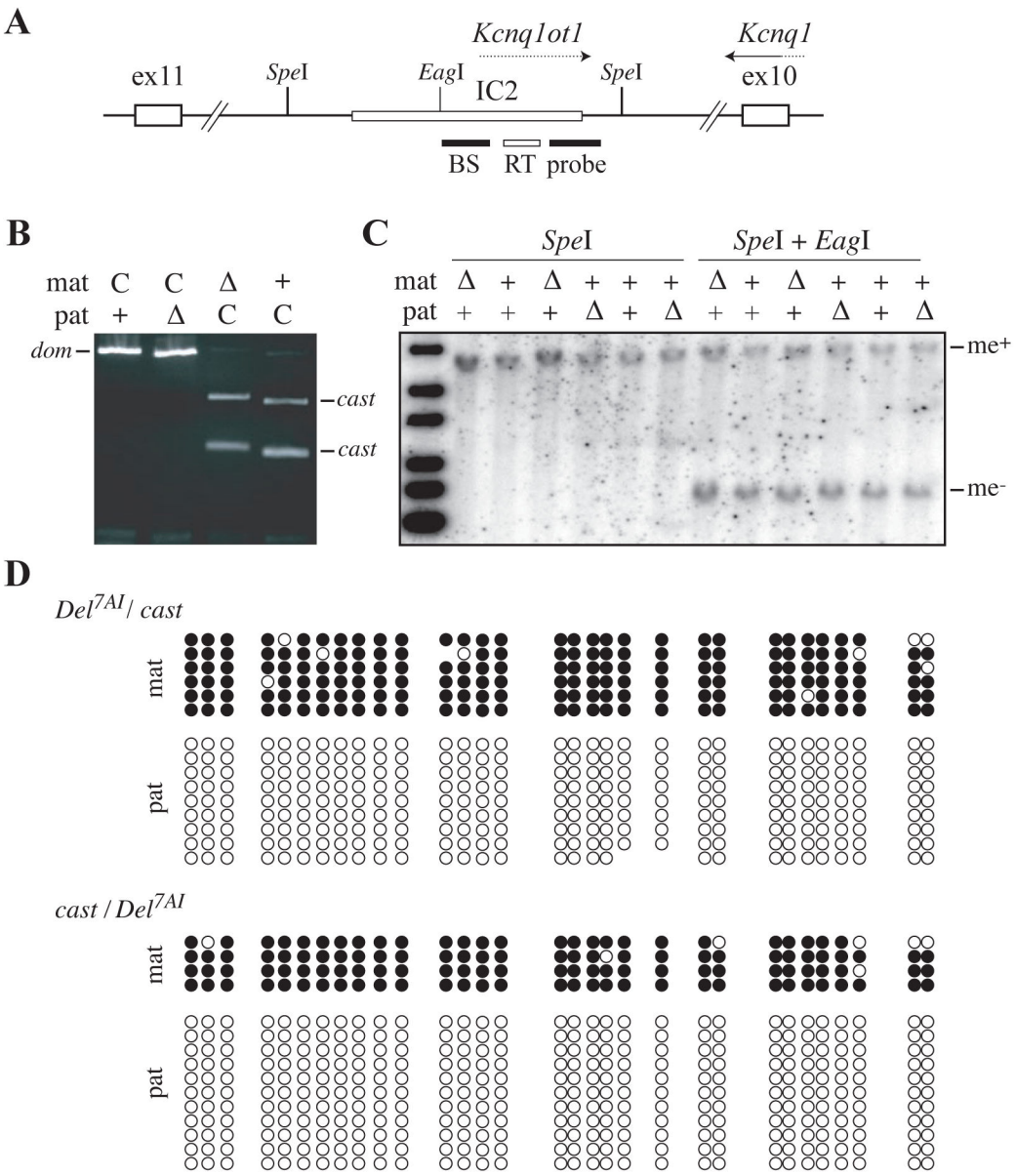


**Figure 6. Imprinting at IC2 in reciprocal *Del*$^{7AI}$ heterozygotes**

Expression and methylation imprinting at IC2 were analyzed in reciprocal heterozygotes for the *Del*$^{7AI}$ allele. (**A**) Diagram of the IC2 region, located within the intron 10 of *Kcnq1*, showing the region amplified by RT-PCR to analyze *Kcnq1ot1* expression in B (RT), the position of the genomic probe used in C (probe) and the 335-bp sequence containing the 31 CpG sites analyzed in D (BS). (**B**) Allele-specific RT-PCR analysis of embryonic *Kcnq1ot1* expression. Maternal (mat) and paternal (pat) alleles are as follows: C, wild-type *castaneus*; +, wild-type *domesticus*; and Δ, *Del*$^{7AI}$. An expressed *Stu*I RFLP was used to distinguish the *castaneus* (*cast*) from the *domesticus* (*dom*) *Kcnq1ot1* variants. (**C**) DNA methylation analysis by Southern blotting of genomic DNA digested with *Spe*I and the methylation sensitive restriction enzyme *Eag*I. Maternal (mat) and paternal (pat) alleles are identified as wild-type (+) or *Del*$^{7AI}$ (Δ). Also shown are the positions of methylated (me+) and

unmethylated (me-) *Spe*I fragment. (**D**) Allele-specific DNA methylation analysis by sodium bisulfite sequencing. The central region of the IC2 DMR was analyzed in reciprocal $Del^{7AI}$ heterozygotes carrying SNPs allowing the identification of the parental alleles. Methylated CpG sites are shown in black, unmethylated sites in white, and omitted sites denote sequencing ambiguities.

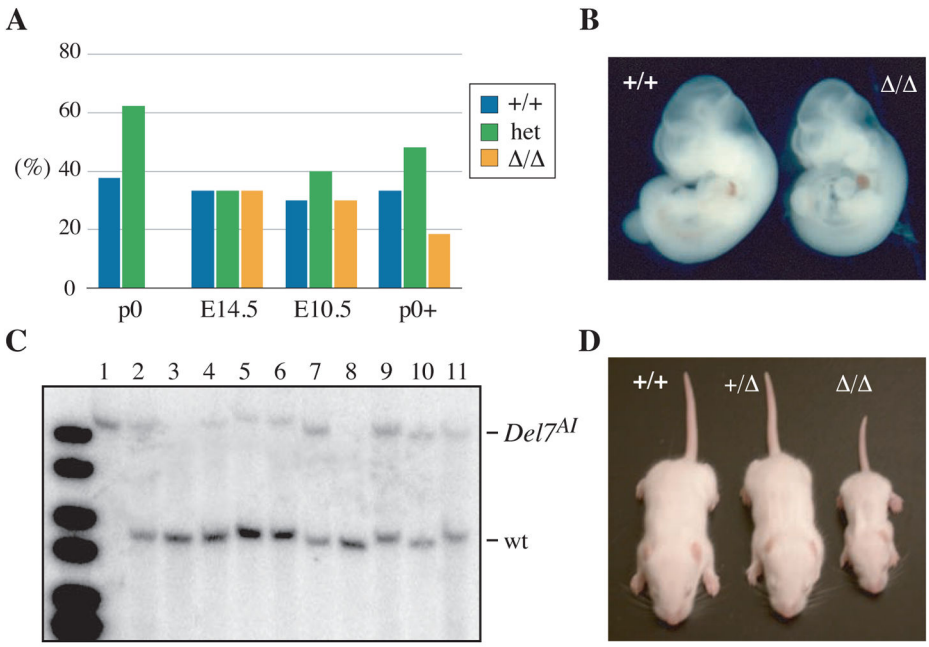


**Figure 7. The embryonic lethality of *Del*$^{7AI}$ homozygotes is pharmacologically rescued by provision of L-DOPA in utero**

(**A**) Live progeny from heterozygous crosses expressed in percentage (%) of wild-type (+/+), *Del*$^{7AI}$ heterozygotes (het) and *Del*$^{7AI}$ homozygous mutants (Δ/Δ) recovered at birth (p0) or at post-implantation embryonic stages (E14.5 and E10.5). Homozygous mutants were rescued to term when the pregnant +/*Del*$^{7AI}$ heterozygous female was provided with L-DOPA in her drinking water during gestation (p0+). (**B**) Wild-type (+/+) and homozygous mutant (Δ/Δ) E10.5 embryos from a heterozygous cross. (**C**) Southern blot analysis of tail genomic DNA from live progeny of heterozygous crosses. Samples 1 to 4 are from a mother treated with L-DOPA, sample 1 is from a rescued homozygote. The expected *Eco*RV bands are 5.2 kb for wild-type and 9.7 kb for *Del*$^{7AI}$. (**D**) Picture of 12-day old pups from a heterozygous cross with L-DOPA treatment.